Dysprosium-Radical Based Single-Molecule Magnet Containing a Seven Coordinate Dy(III) Ion: A System for *ab initio* Study

Saroj Kumar Kushvaha,[a] Prathap Ravichandran,[a] Chen Dan,[b] Liviu Ungur,*[b] Nithin Suryadevara,[c] Mario Ruben,*[c] and Kartik Chandra Mondal*[a]

Dedicated to Prof. P. S. Mukherjee on the occasion of his 50th birthday.

Single–ion magnets (SIMs) possessing a Dy(III) ion have recently attracted huge scientific attention. Herein, we report on a Dy(III)-radical single–molecule magnet containing a seven-coordinate Dy(III) ion with an O_3N_3Cl donor set. The frequency–dependent slow relaxation of magnetization has been observed below 8 K. DC magnetic studies have shown the presence of weak antiferromagnetic coupling between the Kramers ion (Dy(III), $J = 15/2$) and the ligand-centered radical electron ($S = 1/2$) which was confirmed by multifunctional CASSCF calculations.

Introduction

The materials that display the magnetic memory effect have become a part of everyday life in electronic devices.[1] These molecular materials possess a special class of ions in which desired magnetism originates from individual molecular complex due to unique electronic and structural aspects.[2] The magnetic properties can be improved by tuning them. The molecular lanthanides complexes are perfect candidates as materials for molecule based future electronic devices taking the advantage of magnetic and optical properties.[1c] The dependency on such magnetic materials is increasing daily due to the ever–increasing demand for data–storing and data-processing devices.[3–4] However, the data–storage capacity of the traditional magnetic materials has achieved a limit. Therefore, it is necessary to replace the present–day magnetic materials from the devices with precise magnetic molecules/complexes to increase their storage capacity.[1] In this regard, single-molecule magnets (SMMs) are the potential candidates for high-density data storage applications in which the magnetic memory effect originates at the molecular level. However, data storage in such SMMs has not been possible at room temperature. For example, the highest achieved temperature for blocking spin relaxation is only up to 80 K in a Dy(III)-metallocene cation.[5] Since it is possible to replace a magnetic domain with a tiny metal complex (i.e. SMM), it increases the data storage capacity by several thousand times. Scientists continuously strive to synthesize such complexes that can show magnetic memory effect at ambient temperature.[6–7] As a result, this field has received a captivating attention and further achieved a huge progress since the first report of a Mn_{12}-Ac SMM by Sessoli et al in 1990[8] following which thousands of metal complexes[6–8] with different paramagnetic metal ions have been synthesized, characterized and studied for their magnetic measurements and theoretical calculations.[9] A steady shift from the synthesis of high spin and high nuclearity metal complexes to low nuclearity or even single metal ion containing complexes has been noticed over the past one and half decades.[10] The 'philosophical evolution' in this field has been majorly centred around Dy(III) ion due to its desirable electronic properties.[11–12] First, the $4f^9$ ground electronic configuration of the lanthanides have a rather short-radius, preventing strong covalent bonding with the ligands. Following Hund's rules, the ground state of this ion is $^6H_{15/2}$, offering $2J+1 = 16$ energy levels which can be tuned by ligand environment to a large extent. The axial ligand field allows to preserve the pure rotational symmetry of the energy states, preserving their m_J quantum numbers. It came out that many Dy(III) compounds often possess a dominant ligand field environment, which stabilises the Kramers doublet with $m_J = \pm 15/2$ character in the ground state. Therefore, Dy(III)-containing complexes often show magnetic bistability, leading to SMM behaviour.[6–7] Dy(III) ion often possesses a huge uniaxial single-ion magnetic anisotropy with a set of axially coordinating ligands due to its oblate type of electron density distribution.[13] Therefore, different ligands have been employed to synthesize complexes with variable geometry and study the effect of the ligand field on the relaxation dynamics.[14]

[a] *Dr. S. Kumar Kushvaha, P. Ravichandran, Dr. K. Chandra Mondal*
Department of Chemistry, Indian Institute of Technology Madras, Chennai India.
E-mail: csdkartik@iitm.ac.in

[b] *C. Dan, Dr. L. Ungur*
Department of Chemistry, National University of Singapore.
E-mail: chmlu@nus.edu.sg

[c] *Dr. N. Suryadevara, Prof. Dr. M. Ruben*
Institute of Quantum Materials and Technologies (IQMT), Karlsruhe Institute of Technology (KIT), Hermann-von-Helmholtz-Platz 1, 76344 Eggenstein-Leopoldshafen, Germany.
E-mail: mario.ruben@kit.edu

More than a decade ago,[15] Long et al. have shown that coupling of Dy(III) ions with radical electrons can remove the degeneracy of the ground state of a Dy(III) ion, preventing zero–field quantum tunnelling of magnetization (QTM) in $(L)_nLn_2(N_2^{3-})$ system (L=N(TMS)$_2$[15] or Cp*).[16–17] Similarly, Wang et al. have isolated bimetallic azafullerene $Dy_2@C_{79}N$ wherein multiple magnetic centres inside the confined inner space of a fullerene interact ferromagnetically, hence, enabling $Dy_2@C_{79}N$ to be a favourable SMM with a large energy barrier of U = 669 K.[17b–c] Since 4f electron are localized in nature; therefore, they cause weak exchange interactions; however, introducing radical bridges can induce stronger exchange coupling. Liu et al. reported a redox-active SMM, $Ln_2@C_{80}(CH_2Ph)$ (Ln=Tb, Dy, Gd, etc.), wherein the lanthanide spins are radical–bridged by a metal–metal bond.[17d] Notably, $Tb_2@C_{80}(CH_2Ph)$ shows a gigantic coercivity of 8.2 Tesla at 5 K and a high 100 s blocking temperature of magnetization of 25.2 K.[17d] There are several other Ln-radical complexes that have been studied by dynamic magnetic susceptibility measurements.[18–34] Remarkably, a very wide hysteresis loop was displayed by molecular complex $(Cp^{iPr5})_2Dy_2I_3$ possessing a radical electron inbetween two Dy^{III} ions engazing them in strong bonding interaction.[17e] A revelant review by Tang et al have summarised the effect of metal-metal bond in SMMs.[17f]

The most prominent reports include lanthanide complexes with radical ligands such as semiquinoates, nitronyl nitroxides, oxidized phthalocyanines, verdazyls, triazinyls, pyridyl–pyrazines, indigos, super–reduced dinitrogens, dibismuth and bipyrimidyls.[16–32] Their studies have shown that the lanthanide complexes with redox-active radicals and anionic ligands exhibit stronger exchange interactions. The nature of the magnetic coupling between radical electron on aminoxyl radical ligands and lanthanide(III) ions [Ln=Ce to Dy and others] was investigated by Kahn et al nearly two and half decades ago.[17g–i] Moreover, the presence of radicals in these complexes are expected to have a higher barrier and reasonably high blocking temperature. For example, Das et al.[34a] and Long et al.[34b] have utilized radical–anionic iminopyridine ligands[35a–b] to study relaxation dynamics in dysprosium complexes containing pseudo octahedral Dy(III) ions $[Dy(III)(L^{NN\bullet-})_3]$.[34] However, they have not been studied by *ab initio* calculation except the hypothetical non-radical analogue $[Dy(III)(L^{NN})_3]^{3+}$[34] quantum chemical calculation and simulation of hyperfine energy levels of anisotropic Dy-radical system is believed to be quite challenging. Notably, the anionic Ln(III) bis-phthalocyanine complex ($LnPc_2^-$) represents the first family of single–ion magnets (Ln=Dy, Tb, Ho, etc.)[14] which grabbed everyone's attention in the era of 3d-based (especially Mn(III)-based coordination clusters) molecular clusters often displaying SMM behaviour with ground-state spin of as high as possible. Previously, we have studied the anionic $TbPc_2^-$ complex without any radical electron and neutral Tb(III) bis–phthalocyanine ($TbPc_2$) complex containing a radical electron on one of the phthalocyanine-ring (Pc) exploring the different aspects and potential of radical electron containing $TbPc_2$ complexes. neutral $TbPc_2$ complex with a radical electron on the ring could be utilized as qudits.[36] Herein, we report on an antiferromagnetically coupled redox-active Dy(III)-radical based single-molecule magnet (SMM) $[Li(I)Dy(III)(L^1)(L^{NN\bullet-})(Cl)]\cdot$tol (**1**) containing a seven coordinate Dy(III) ion with an O_3N_3Cl donor-set with a radical-anionic iminopyridine ligand and another co–ligand. The experimentally obtained data has been well correlated with the computational studies.

Results and Discussion

Syntesis

Anhydrous $DyCl_3$, iminopyridine ligand (**L^{NN}**) and lithiated salt of co–ligand (**Li–L^1**) were taken in a 3 : 3 : 4 molar ratio in a Schlenk flask containing 10 mL of dry THF, and the stirring was started in the glovebox (Scheme 1). After 5 min of stirring, one equivalent (w.r.t. **L^{NN}**) of K metal was added to the reaction mixture. The subsequent stirring produced a dark green–coloured reaction mixture, which was stirred for 10 hours. Then, the reaction mixture was dried under a vacuum by removing the THF solvent. After that, 20 mL of dry toluene, a less polar solvent than THF, was added to the green residue and the solution was further stirred for 10 min and concentrated under vacuum. The concentrated solution was kept in the glovebox at −40 °C for crystallization. The block–shaped green crystals of $[Li(I)Dy(III)(L^1)(L^{NN\bullet-})(Cl)]\cdot$tol (**1**) suitable for single crystal XRD were formed in a week. The yield was calculated to be 46% based on $DyCl_3$. Anal (%). calcd for complex **1** ($C_{65}H_{78}ClDyLiN_4O_4$) : C, 65.92; H, 6.64; N, 4.73 Found: C, 65.86; H, 6.25; N, 4.66. UV-vis bands at 365 and 690 nm. X band EPR at room temperature and cyclic voltammetry (CV) studies of complex **1** have been given in the SI.

Structural Description

The complex $[Li(I)Dy(III)(L^1)(L^{NN\bullet-})(Cl)]$.tol (**1**) crystallizes in the triclinic *P*-1 space group. The asymmetric unit contains one Dy^{3+} ion, one Li^+ ion, a chlorine atom, three ligand molecules and a co-crystallized toluene molecule. The Dy^{3+} ion is septa-coordinated with coordination environment N_3O_3Cl. The coordination sphere around the Dy^{3+} ion can be described as capped trigonal prism (CTPR-7) geometry according to SHAPE 2.1 analysis (see Table S4).[37a] The Dy–O bond distances are in the range of 2.240(3)–2.671(4) Å. The Dy–Cl bond length is

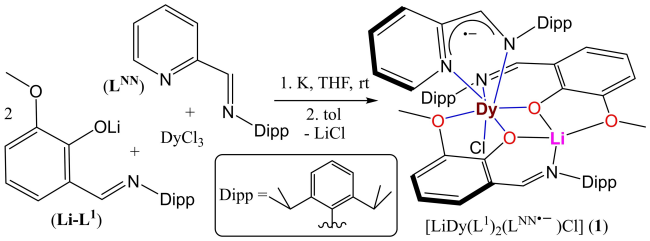

Scheme 1. Synthetic route of Dy-radical complex (**1**) containing a seven-coordinate Dy(III) ion. Dipp = 2,6-diisopropylphenyl.

2.5814(16) Å. The Dy–N_{LNN} bond distances of **1** are 2.387(5)–2.435(5) Å. The Dy–N bond distances in the pseudo-octahedral Dy(III)-radical complex reported by Trifonov et al. and Shanmugam et al. are in the range of 2.392(2)–2.4653(1) Å.[34] These bond distances match with the system discussed in this paper. The Li^+ ion is tetra-coordinated with an O_3N coordination environment, which adopts distorted square planar geometry. The Dy^{3+} and Li^+ ions are connected through two O-bridges, forming Dy–O–Li bond angles of 102.2(3) and 103.1(3)°.

The Dy–N_{Py} distance in the radical anionic ligand is 2.435(5) Å, and the Dy–N_{imine} bond length is 2.387(5) Å. The bond distances within the planar diimino-fragment N_{Py}–C–C–N_{imine} backbone in **1** are consistent with the radical, anionic form of the $L^{NN\bullet-}$ ligand. Here, the bond distances N_{Py}–C, C–C, and C–N_{imine} are 1.381(9), 1.400(10) and 1.339(8) Å, which matches with the previously reported bond distances of L^{NN} radical anionic ligand (Figure 1 and Tables S1–S2).[34–35]

Magnetic Properties

The dc magnetic susceptibility measurements were performed on a powdered sample obtained by grinding dark blue–black single crystals of [Li(I)Dy(III)(L)($L^{NN\bullet-}$)(Cl)]·tol (**1**·tol) in the temperature range of 2–300 K under the external magnetic field (1 kOe).[14–27,34] Complex **1**·tol shows a χT value of 13.2 $cm^3 K mol^{-1}$ at 300 K, consistent with the previously reported SMMs containing a single Dy^{3+} ion.[15a–b–34b] The χT product of [Dy(III)($L^{NN\bullet-}$)$_3$]·0.5tol is 14.0 $cm^3 K mol^{-1}$ at 300 K.[34b] This may also be due to the solid-state effect.[15c] Also, the experimental χT value is comparable to the theoretically calculated value of 14.54 $cm^3 K mol^{-1}$ for a non–interacting Dy^{3+} ion (g = 4/3 and $^6H_{15/2}$) and one mono–radical ($S = {}^1/_2$, g = 2).[6–27,34] Upon cooling, the complex exhibited a decrease of $\chi_M T$ to reach the values of 7.95 $cm^3 K mol^{-1}$ at 2 K (Figure 2, left), which can be attributed to the thermal depopulation of the m_J levels, which is an inherent property of the individual dysprosium centres.[6] Also, it is visible that the sharp decrease in $\chi_M T$ value below 50 K indicates the presence of the antiferromagnetic interaction[16–17,34] between the Dy^{3+} and the radical and was confirmed by calculations (vide infra). The χT product of [Dy(III)($L^{NN\bullet-}$)$_3$] remained constant from 300 to 30 K and below which it went down to ~9.5 $cm^3 K mol^{-1}$ at 1.8 K from 15.29 $cm^3 K mol^{-1}$ at 300 K, suggesting antiferromagnetic interaction between Dy(III) and radical electron on L^{NN} ligand is stronger in **1**.[34a] Point to be noted that χT product fell to ~5.5 $cm^3 K mol^{-1}$ at 1.8 K from 14.0 $cm^3 K mol^{-1}$ at 300 K [Dy(III)($L^{NN\bullet-}$)$_3$]·0.5 tol.[34b] It suggests that lattice toluene can cause significant perturbation to the magnetic parameters.[34]

The field dependencies of magnetization were measured at 2 K, 3 K and 5 K for **1**·tol (Figure 2, right). The magnetization approached saturation; however, the complex did not reach saturation at 7 T due to interplay with the low-lying excited states.[6] The dynamic behaviour of magnetization in complex **1**·tol was investigated by *ac* magnetic susceptibility measurements using an oscillating ac field of 3.5 Oe at 1–1500 Hz frequencies to probe the presence of slow relaxation of magnetization.[6–27] The *ac* susceptibility contains the in-phase (χ_M') and the out-of-phase (χ_M'') components and were measured as a function of temperature (T) and as a function of the ac frequency (ν), as shown in Figure 3. This complex **1**·tol displays signals in the out–of–phase component (χ_M'') of the *ac* magnetic susceptibility without an externally applied *dc* field, indicating strong frequency dependence and slow magnetisation relaxation.[16–17] The maximum intensity of the out–of–phase components gradually decreases with increasing temperature. The maximum of the signal shifts from low frequency to high frequency, indicating strong frequency dependence up to 7.2 K. Both the curves plotted were fitted together using a generalized Debye model[37b] through which the relaxation times (τ) were yielded at particular temperature using the equation $\tau = 2\pi\nu$. The values of α are in the range 0.5–0.6 indicating the presence of more than one relaxation pathway operating at these temperatures. This can also be viewed on Cole-Cole plots obtained within the temperature of 2–7.2 K as they show asymmetric semicircular shapes implying multiple pathways of relaxation (Figure 4). The α values and other fitting parameters at different temperatures have been given in the ESI (Table S3).

The Arrhenius graph of **1**·tol, plotted using the natural logarithm of the relaxation time (ln τ_0) and the inverse of temperature (1/T), showed a curvature indicating that the dynamics cannot be modelled using a simple Orbach mechanism. Here, the data could be fitted using thermally activated Orbach [$\propto \exp(-U_{eff}/k_BT)$] and Raman processes ($\propto T^n$), according to the equation (1).

$$\tau^{-1} = \tau_0^{-1} e^{\frac{U_{eff}}{k_B T}} + CT^n \quad (1)$$

Where τ is the inverse of the *ac* frequency, T is the temperature of the maximum in the *ac* signal, U_{eff} is the effective energy barrier, k_B is Boltzmann's constant, and C and τ_0

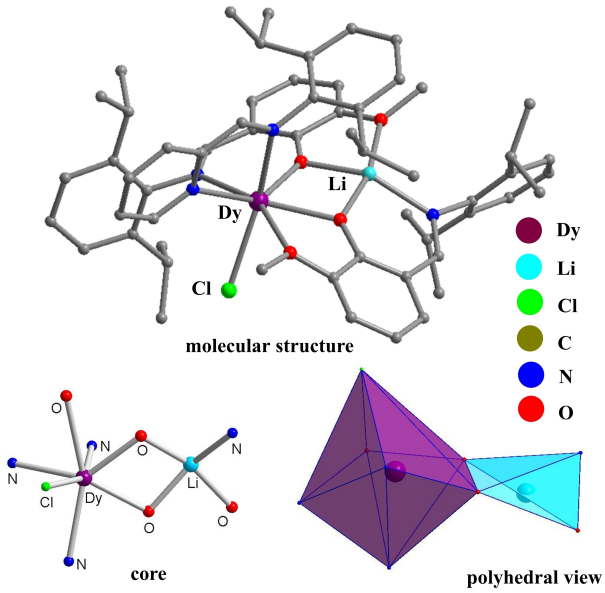

Figure 1. The molecular structure of the complex [Li(I)Dy(III)(L^1)($L^{NN\bullet}$)(Cl)]·tol (**1**·tol) and its core structure.

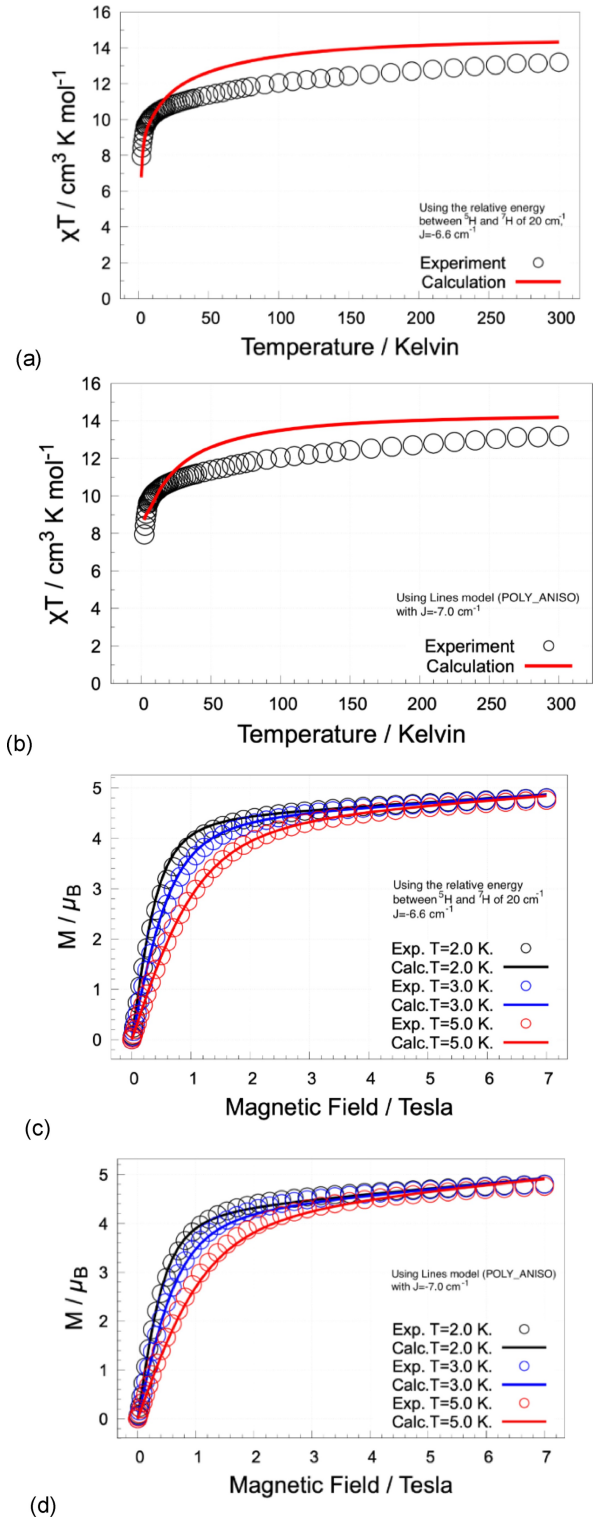

Figure 2. The χ_MT versus T (top; H = 1 kOe; a–b) and M versus H (bottom; c–d) plots of complex **1**·tol. Comparison between calculated and measured magnetic susceptibility (a, b) and molar magnetization (c, d) of **1**·tol, using the two methods described in the text. Powdered samples were obtained by grinding the single crystals **1**·tol for magnetic measurements.

are the fitting parameters of the different relaxation mechanisms.[6–28]

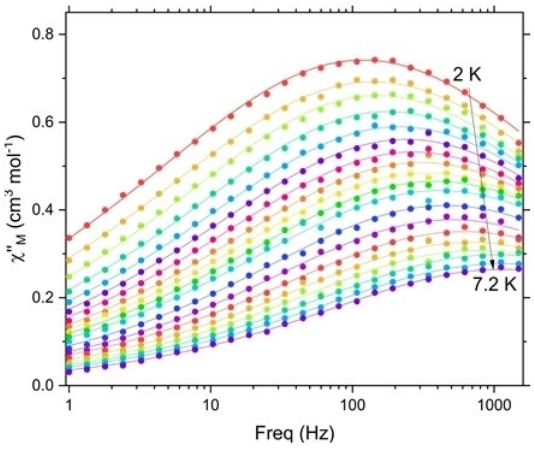

Figure 3. In-phase (χ_M') vs frequency (top) and out-of-phase (χ_M'') vs frequency (bottom) components of ac magnetic susceptibility of complex **1**·tol.

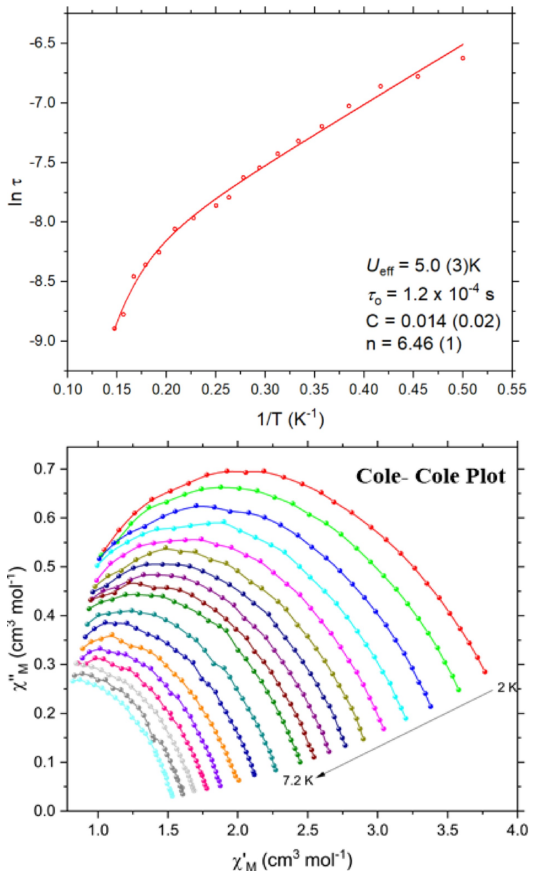

Figure 4. Arrhenius plot (Top) of relaxation time vs 1/*T* and Cole-Cole plot (bottom) of complex **1**·tol.

The fitting using the above equation in the 2–7 K temperature range resulted in a low energy barrier of U_{eff} = 5 K and pre-exponential factor of $\tau_0 = 1.2\times10^{-4}$ s with $C = 0.014$, $n = 6.46$ for 1 tol. However, to confirm the QTM contribution, fitting of the data was performed by including the QTM parameter using the following equation (2) which has showed negligible QTM contribution ($\tau_{QTM} = \sim10^{24}$) (Table 1).

Table 1. Different fitting parameters of AC data of complex **1**.

	without QTM	with QTM
	$\tau_0 = 1.2\times10^{-4}$	$\tau_0 = 1.51\times10^{-4}$
U_{eff}	5	4.8
n	6.46	4.9
$\tau_{(QTM)}$	–	6×10^{24}

$$\tau^{-1} = \tau_0^{-1} e^{\frac{U_{eff}}{K_B T}} + CT^n + \tau_{QTM}^{-1} \quad (2)$$

Previously reported complexes [Dy(III)($L^{NN\bullet-}$)$_3$] and [Dy(III)($L^{NN\bullet-}$)$_3$]·0.5 tol having a six-coordinate Dy(III) ion (with distorted octahedral coordination geometry) possess additional QTM process. The reversal of magnetization happens via Orbach, Raman and QTM processes.[34] The thermal energy barrier of the latter is reported to be 28/34 cm^{-1} in the absence/presence of the external *dc* magnetic field of 1 kOe.[34b] The former complex[34a] possesses two relaxation processes (fast and slow), having energy barriers of 23.5 and 10.3 cm^{-1}, respectively. The relaxation time for the Orbach process is significantly slower in **1**·tol in the absence of the external *dc* field. The molecular complexes are stacked in solid material with some shorts of overall attraction inter-molecular forces. The phonon vibrations for the corresponding slow relaxation of magnetization can pass from one molecular complex to it neighbouring complexes leading to a more complicated situation.[34,35c]

Ab Initio Calculations

Further insight into the electronic structure and properties of complex **1** was obtained through *ab initio* and density functional theory (DFT) calculations. *Ab initio* multireference calculations were used to derivate the electronic energy states and crystal field splitting,[38–39] while the broken symmetry DFT calculations were employed to derivate the magnetic exchange interaction.[40] The low-lying electronic structure of complex **1** can be understood as the spin coupling between the ground state of the Dy^{3+} ion (^{6}H term) and the radical electron (^{2}S state), giving rise to a high-spin term (^{7}H, Dy–R ferromagnetic coupling) and a low-spin term (^{5}H, Dy–R antiferromagnetic coupling). Excited terms also undergo similar exchange coupling to give rise to ^{7}F and ^{5}F terms. The energy separation of the high-spin and low-spin states is due to the magnetic exchange interaction. It is expected to be significantly smaller than the crystal field splitting of these terms. Figure 5 shows the energy spectrum of the low-lying electronic structure of complex **1**, as obtained in the calculations. Ab initio multiconfigurational calculations were based on the full molecular structure obtained in X-ray measurements without computational structural optimization. RASSCF/RASSI calculations were performed on an active space of 18 electrons in 17 orbitals.[41] All atoms were described with the ANO-RCC basis sets, which include relativistic corrections for core orbitals. Dy and all closely spaced atoms were described with large VTZP basis sets, while distant atoms were described with medium VDZP basis.[42] All molecular orbitals and low–lying excitations were evaluated within Complete Active Space Self Consistent Field (CASSCF) calculations.[43] The active space included the 5 $s^2$5p^6 shells in RAS1 space, 4f^9 and the radical in RAS2 space and the 5d shell in RAS3 space.[44] Configurations with a maximum of 2 holes in RAS1 and 2 electrons in RAS3 were allowed. The terms H and F of high–spin and low–spin configurations were computed (18 roots for each spin value) and were subsequently mixed by the spin–orbit coupling in RASSI. The latter interaction was accounted for within a one-center mean-field approximation (AMFI). SINGLE_ANISO and POLY_ANISO software described magnetic properties based on the calculated low-lying states.[45–50] The obtained crystal-field splitting of the ^{5}H and ^{7}H terms (Figure 5, left) and subsequently of the $^5H_7$ and $^7H_8$ spin–orbit multiplets are given in Table 2. The anisotropic axis on the Dy-centre has been shown in Figure 5, right with dotted red lines. Broken-symmetry DFT calculations were done using ORCA quantum chemistry software[51] to find the strength of the magnetic interaction between the radical and the lanthanide ion. For these purposes, the **Gd–1** substituted model of the original compound **1** was employed, where the Gd ion computationally replaced the Dy. The metal substitution stems from the near-orbital degeneracy of the low–lying state of the Dy^{3+} site, making it unsuitable for DFT description. The ground state of the Gd^{3+} ion is ^{8}S, non-degenerate, and therefore suitable for DFT.[52] BP functional was employed alongside def2-TZVP basis sets and very tight convergence thresholds. Calculated exchange couplings obtained for Gd–R were rescaled by coefficient 7/5 to match the exchange Hamiltonian $\widehat{H}_{ex} = -J\widehat{S}_{Dy}\widehat{s}_{Rad}$ ($\widehat{S}_{Dy} = \frac{5}{2}, \widehat{S}_{Gd} = \frac{7}{2}$). The calculated magnetic ex-

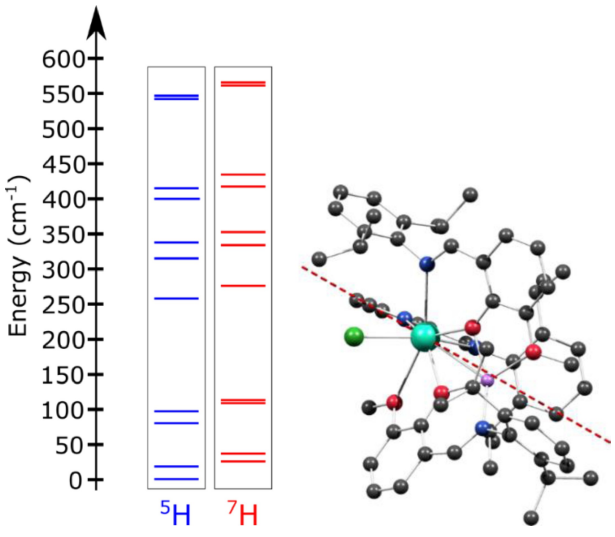

Figure 5. Low–lying term energy structure of complex **1**. Note that the crystal field splitting of the ^{7}H and ^{5}H terms have a similar pattern but are not identical. The relative energy separation between ^{5}H and ^{7}H was left as an adjustable parameter with a best–fitted value of about 20 cm^{-1}, corresponding to an effective $J = -6.7$ cm^{-1} (left). The Red dashed line shows the orientation of the main magnetic axis in the ground state of **1** in the molecular frame. Color scheme: Dy-cyan, Cl-green, C-dark grey, Li-pink, N-blue. Hydrogen atoms are not shown for clarity (right).

Table 2. Low-lying energy states for **1**, $\mathbf{1}^{+}$ and of the radical alone (in cm^{-1}).

No radical, Cation $\mathbf{1}^{+}$, ^{6}H term	No radical, Cation $\mathbf{1}^{+}$, $^{6}H_{15/2}$ multiplet	Neutral **1**, ^{7}H term	Neutral **1**, $^{7}H_{8}$ multiplet	Neutral **1**, ^{5}H term	Neutral **1**, $^{5}H_{7}$ multiplet	Excited states on radical alone
0.0	0.0	0.0	0.0	0.0	0.0	10476.4
15.3	0.0	16.6	0.4	23.3	3.0	13447.1
108.6	63.8	80.5	16.1	71.2	19.5	16631.7
143.0	63.8	86.8	16.8	92.2	23.0	21950.9
230.7	113.8	255.5	133.0	257.9	156.2	22073.7
266.9	113.8	323.3	134.8	327.5	171.8	23035.1
310.1	184.5	345.4	180.4	349.9	215.5	23566.8
417.2	184.5	419.1	195.4	424.1	244.8	23994.2
444.2	221.0	425.4	228.8	425.5	251.4	24997.2
498.4	221.0	558.8	243.1	557.3	273.9	25453.4
518.8	277.8	563.4	264.4	562.1	295.9	
	277.8		290.5		405.5	
	377.2		294.7		407.4	
	377.2		403.2		466.2	
	412.4		404.6		468.3	
	412.4		453.8			
			454.5			

change value depends on the applied formula (Noodleman, Bencini & Gatteschi or Yamaguchi) and ranges between −4.3 and $-12.3\ cm^{-1}$. Similar exchange values were obtained with other basis sets and DFT functionals.[41d] The extracted $J_{Gd\text{-}radical}$ value of previously reported $[Gd(L_{NN}^{\bullet-})_3]$ is $-1.85\ cm^{-1}$ (antiferromagnetic coupling) with radical–radical coupling constant of $-111.9\ cm^{-1}$.[34a] Kahn et al have reported $J_{Gd\text{-}rad} = +6.1\ cm^{-1}$ (ferromagnetic coupling) for [Gd(aminoxyl radical)$_2$(NO$_3$)$_3$] with the radical-radical coupling constant (J') of $-7.0\ cm^{-1}$.[17g] Ferromagnetic coupling was also observed in Dy-analogue.[17h–i] Gatteschi et al also have reported ferromagnetic coupling for Gd(III)-radical magnetic interaction.[17b,33b–c]

The spin density distribution of the radical alone was found using the spin-unrestricted DFT calculation on the **Lu–1**, which was obtained by substituting the Dy with diamagnetic Lu in the calculation. Figure 6 shows the spin density distribution of the radical in this compound. Time-dependent DFT calculations evaluated excited states of **Lu–1**, and it was found that they lie about $10400\ cm^{-1}$ higher in energy than the ground state.

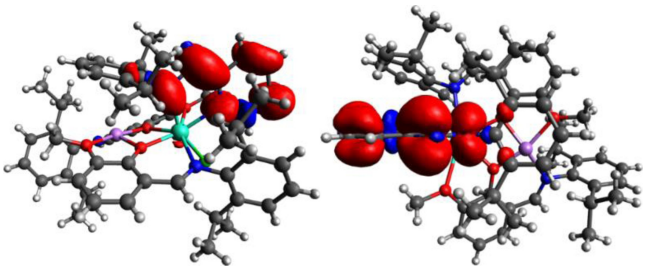

Figure 6. Spin density distribution of the radical alone, as computed for **Lu–1**.

As such, we may conclude that excited states on the radical do not participate significantly in magnetic exchange. Two semi–ab initio approaches were employed to extract the magnetic exchange using the measured magnetism. The first method consisted of adjusting the relative energy difference between the ^{7}H and ^{5}H terms (at their barycenter) and mixing them by spin-orbit coupling in RASSI.[41] The crystal–field splitting of these terms and their wave functions were kept as in the original *ab initio* calculations (as listed in Table 2). The resulting spin-orbit states were used for the description of the magnetism of compound **1** using the SINGLE_ANISO program.[45–49]

The best–fitting parameter was $-20\ cm^{-1}$, corresponding to a J value of about $-6.7\ cm^{-1}$. As an alternative to the above method, the magnetic properties of **1** were described within the Lines model by employing POLY-ANISO software. We used the *ab initio* results for the cation $\mathbf{1}^{+}$ for these purposes, while the radical was modelled as isotropic $S = 1/2$. The molar magnetization and magnetic susceptibility were best described using the $J = -7.0\ cm^{-1}$ for the mentioned exchange Hamiltonian, in close agreement with the one predicted by the first method. Figure 2 shows the comparison between measured and calculated magnetism for both methods. A similar theoretical calculation on previously reported $[Dy(L_{NN}^{\bullet-})_3]$[34] has not been carried out. However, $J_{Dy\text{-}rad}$ is estimated to be $-1.32\ cm^{-1}$ based on the $J_{Gd\text{-}rad}$ extracted from the fitting of χT vs T plot ($-1.85\ cm^{-1}$).[33b–c,34a] It is noted that the agreement between measured and calculated powder magnetization is quite good, while the description of measured susceptibility is less satisfactory. Based on the obtained low-lying exchange eigenstates, the blocking barrier plot is built by arranging energy

states as a function of their intrinsic magnetic moment along the quantization axis (i.e. the main axis of ground KD of Dy site, the magnetization blocking barrier of **1**) (Figure 7).

The fitting of the AC susceptibility data employing equations (1) and (2) showed that the effective energy barrier for the Orbach process is nearly 5 cm^{-1}. However, the overall reorientation of the magnetization complex **1** is most possibly accompanied by other processes as well (Raman and QTM). Our *ab initio* calculation revealed that the corresponding energy barrier for the Orbach process is likely to be ~15 cm^{-1} (first excited state). The deviation can be attributed to the interplay between all these processes. A similar problem has been recently addressed in dipotassiumtetrachloride-bridged dysprosium metallocenes.[10b] In past the authors were not regeularly discussing the eorror bars in the fitting of the data which has been addressed in the report of the dysprosium metallocenes.[10b]

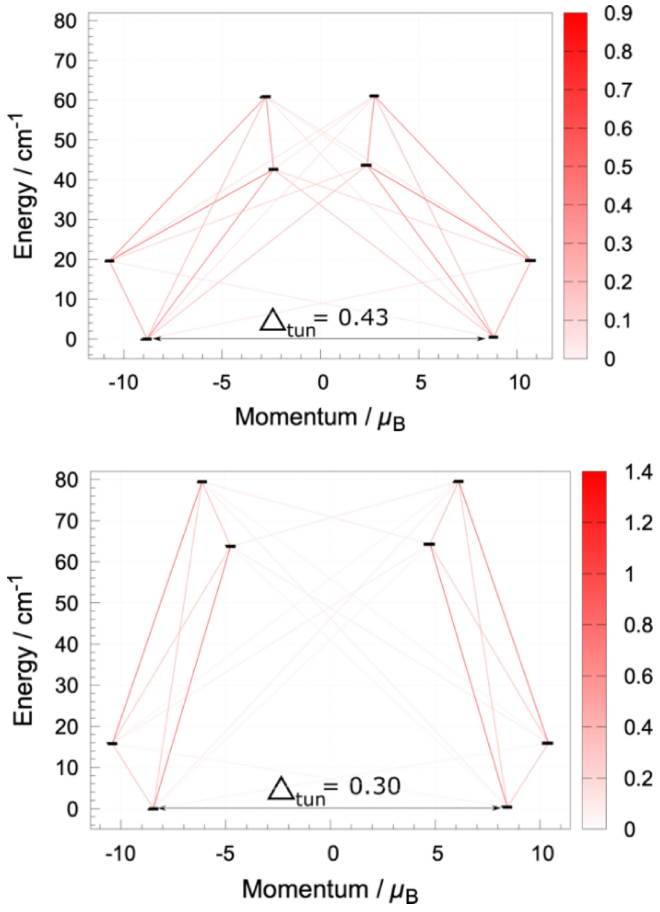

Figure 7. Blocking barrier for **1** as predicted by the two computational approaches employed. (top) the method using the relative energy between ^{5}H and ^{7}H terms of 20 cm^{-1}, $J=-6.6$ cm^{-1}; (bottom) the Lines model (POLY_ANISO) with $J=-7.0$ cm^{-1}. Because of the significant value of tunnel splitting predicted by either method, the molecule is not a performant single-molecule magnet, in line with experimental evidence.

Conclusions

In conclusion, we have synthesized and isolated an air and moisture-sensitive Dy(III)-mono-radical coordination complex containing a Dy(III) ion with seven coordination numbers. The radical electron of the anionic NN-donor ligand is weakly antiferromagnetically coupled with the Dy(III) ion. The slow relaxation of magnetization has been displayed below 8 K with a relatively high relaxation time ($\tau_0=1.2\times10^{-4}$ s). *Ab initio* calculations explained the low-lying energy structure and magnetism, revealing the origin of the fast-magnetic relaxation in this compound, unlike previously studied Dy(III)- based SIM with seven coordination numbers.[11] Our multi-reference/functional CASSCF calculations rationalize the experimental results quite well. Our investigation shades deeper insight into Dy-radical based SMM, especially to two closely relevant Dy(III)-tri-radical complexes.[34]

Supporting Information

The authors have cited additional references within the Supporting Information. Supporting Information contains synthesis, elemental analysis, crystallographic data and tables, coordinates, and other computational details.

Acknowledgements

S. K. K. thanks, IIT Madras, for SRF. K. C. M. thanks SERB for the ECR grant (ECR/2016/000890) and IIT Madras for the seed grant. L. U. acknowledges the financial support of the research projects R-143-000-A65-133, R-143-000-A80-114, and A-8000017-00-00 of the National University of Singapore. *Ab initio* calculations were done on the ASPIRE-1 cluster (www.nscc.sg) under the project 11001278.

Conflict of Interests

The authors declare no conflict of interest.

Data Availability Statement

The data that support the findings of this study are available in the supplementary material of this article.

Keywords: Metal–radical system · Dy(III) single–molecule magnet · Suppression of QTM · Magnetic studies · CASSCF calculation

[1] a) R. A. Murphy, J. R. Long, T. D. Harris, *Commun. Chem.* **2021**, *4*, 70; b) M. Mannini, F. Pineider, C. Danieli, F. Totti, L. Sorace, P. Sainctavit, M. A. Arrio, E. Otero, L. Joly, J. C. Cezar, A. Cornia, R. Sessoli, *Nature* **2010**, *468*, 417; c) K. Bernot, C. Daiguebonne, G. Calvez, Y. Suffren, O. Guillou, *Acc. Chem. Res.* **2021**, *54*, 427.

[2] K. M. Krishnan, *Fundamentals and Applications of Magnetic Materials* OUP Oxford; 1st edition (18 August 2016); ISBN-13: 978-0199570447.
[3] D. A. Thompson, J. S. Best, *IBM J. Res. Dev.* **2000**, *44*, 311.
[4] O. Gutfleisch, M. A. Willard, E. Brück, C. H. Chen, S. G. Sankar, J. P. Liu, *Adv. Mater.* **2011**, *23*, 821.
[5] F. S. Guo, B. M. Day, Y. C. Chen, M. L. Tong, A. Mansikkamäki, R. A. Layfield, *Science* **2018**, *362*, 1400.
[6] a) J. L. Liu, Y. C. Chen, M. L. Tong, *Chem. Soc. Rev.* **2018**, *47*, 2431; b) A. Dey, P. Kalita, V. Chandrasekhar, *ACS Omega* **2018**, *3*, 9462; c) G. Cucinotta, M. Perfetti, J. Luzon, M. Etienne, P. E. Car, A. Caneschi, G. Calvez, K. Bernot, R. Sessoli, *Angew. Chem. Int. Ed.* **2012**, *51*, 1606.
[7] a) S. Demir, I. R. Jeon, J. R. Long, T. D. Harris, *Coord. Chem. Rev.* **2015**, *149*, 289; b) S. G. McAdams, A. M. Ariciu, A. K. Kostopoulos, J. P. S. Walsh, F. Tuna, *Coord. Chem. Rev.* **2017**, *346*, 216; c) J. Lu, M. Guo, J. Tang, *Chem. Asian J.* **2017**, *12*, 2772.
[8] a) A. Caneschi, D. Gatteschi, R. Sessoli, A. L. Barra, L. C. Brunel, M. Guillot, *J. Am. Chem. Soc.* **1991**, *113*, 5873; b) R. Sessoli, D. Gatteschi, A. Caneschi, M. A. Novak, *Nature* **1993**, *365*, 141.
[9] a) S. Gómez-Coca, A. Urtizberea, E. Cremades, P. J. Alonso, A. Camón, E. Ruiz, F. Luis, *Nat. Commun.* **2014**, *5*, 4300; b) D. H. Moseley, S. E. Stavretis, K. Thirunavukkuarasu, M. Ozerov, Y. Cheng, L. L. Daemen, J. Ludwig, Z. Lu, D. Smirnov, C. M. Brown, A. Pandey, A. J. Ramirez-Cuesta, A. C. Lamb, M. Atanasov, E. Bill, F. Neese, Z. L. Xue, *Nat. Commun.* **2018**, *9*, 2572.
[10] a) A. Zabala-Lekuona, J. M. Seco, E. Colacio, *Coord. Chem. Rev.* **2021**, *441*, 213984; b) S. Arumugam, B. Schwarz, P. Ravichandran, S. Kumar, L. Ungur, K. C. Mondal, *Dalton Trans.* **2023**, *52*, 15326.
[11] a) Y.-S. Ding, N. F. Chilton, R. E. P. Winpenny, Y. S. Zheng, *Angew. Chem. Int. Ed.* **2016**, *55*, 16071; b) A. B. Canaj, S. Dey, O. Céspedes, C. Wilson, G. Rajaraman, M. Murrie, *Chem. Commun.* **2020**, *56*, 1533; c) A. B. Canaj, S. Dey, C. Wilson, O. Céspedes, G. Rajaraman, M. Murrie, *Chem. Commun.* **2020**, *56*, 12037; d) K. X. Yu, J. G. C. Kragskow, Y. S. Ding, Y. Q. Zhai, D. Reta, N. F. Chilton, Y. Z. Zheng, *Chem.* **2020**, *6*, 1777.
[12] A. B. Canaj, S. Dey, E. R. Mart, C. Wilson, G. Rajaraman, M. Murrie, *Angew. Chem. Int. Ed.* **2019**, *58*, 14146.
[13] a) F.-S. Guo, B. M. Day, Y.-C. Chen, M.-L. Tong, A. Mansikkamäki, R. A. Layfield, *Angew. Chem. Int. Ed.* **2017**, *56*, 11445; b) C. A. P. Goodwin, F. Ortu, D. Reta, N. F. Chilton, D. P. Mills, *Nature* **2017**, *548*, 439.
[14] N. Ishikawa, M. Sugita, T. Ishikawa, S.-Y. Koshihara, Y. Kaizu, *J. Am. Chem. Soc.* **2003**, *125*, 8694.
[15] a) C. G. T. Price, A. Mondal, J. P. Durrant, J. Tang, R. A. Layfield, *Inorg. Chem.* **2023**, *62*, 9924; b) J. D. Rinehart, M. Fang, W. J. Evans, J. R. Long, *Nat. Chem.* **2011**, *3*, 538; c) J. D. Rinehart, J. R. Long, *Chem. Sci.* **2011**, *2*, 2078; d) C. Gao, A. Genoni, S. Gao, S. Jiang, A. Soncini, J. Overgaard, *Nat. Chem.* **2020**, *12*, 213.
[16] a) S. Demir, J. M. Zadrozny, M. Nippe, J. R. Long, *J. Am. Chem. Soc.* **2012**, *134*, 18546; b) S. Demir, M. I. Gonzalez, L. E. Darago, W. J. Evans, J. R. Long, *Nat. Commun.* **2017**, *8*, 2144; c) C. A. Gould, E. Mu, V. Vieru, L. E. Darago, K. Chakarawet, M. I. Gonzalez, S. Demir, J. R. Long, *J. Am. Chem. Soc.* **2020**, *142*, 21197; d) C. A. Gould, L. E. Darago, M. I. Gonzalez, S. Demir, J. R. Long, *Angew. Chem. Int. Ed.* **2017**, *56*, 10103; e) F. Delano, E. Castellanos, J. McCracken, S. Demir, *Chem. Sci.* **2021**, *12*, 15219; f) S. Demir, M. Nippe, M. I. Gonzalez, J. R. Long, *Chem. Sci.* **2014**, *5*, 4701; g) P. Zhang, R. Nabi, J. K. Staab, N. F. Chilton, S. Demir, *J. Am. Chem. Soc.* **2023**, *145*, 9152.
[17] a) Y.-C. Chen, J. L. Liu, W. Wernsdorfer, D. Liu, L. F. Chibotaru, X.-M. Chen, M.-L. Tong, *Angew. Chem. Int. Ed.* **2017**, *56*, 4996; b) C. Benelli, A. Caneschi, D. Gatteschi, L. Pardi, *Inorg. Chem.* **1992**, *31*, 741; c) Wujun Fu, J. Zhang, T. Fuhrer, H. Champion, K. Furukawa, T. Kato, J. E. Mahaney, B. G. Burke, K. A. Williams, K. Walker, C. Dixon, J. Ge, C. Shu, K. Harich, H. C. Dorn, *J. Am. Chem. Soc.* **2011**, *133*, 9741; d) R. Ray, N. A. Samoylova, C.-H. Chen, M. Rosenkranz, S. Chiemenz, F. Ziegs, K. Nenkov, A. Kostanyan, T. Greber, A. U. B. Wolter, M. Richter, B. Buchner, S. M. Avdoshenko, A. A. Popov, *Nat. Commun.* **2019**, *10*, 571; e) C. A. Gould, K. R. McClain, D. Reta, J. G. C. Kragskow, D. A. Marchiori, E. Lachman, E.-S. Choi, J. G. Analytis, R. D. Britt, N. F. Chilton, B. G. Harvey, J. R. Long, *Science* **2022**, *375*, 198; f) Z. Zhu, J. Tang, *Chem. Soc. Rev.* **2022**, *51*, 9469; g) J.-P. Sutter, M. L. Kahn, S. Golhen, L. Ouahab, E. O. Kahn, *Chem. Eur. J.* **1998**, *4*, 571; h) M. L. Kahn, J.-P. Sutter, S. Golhen, P. Guionneau, L. Ouahab, O. Kahn, D. Chasseau, *J. Am. Chem. Soc.* **2000**, *122*, 3413; i) J.-P. Sutter, M. L. Kahn, O. Kahn, *Adv. Mater.* **1999**, *11*, 863.
[18] F. Liu, D. S. Krylov, L. Spree, S. M. Avdoshenko, N. A. Samoylova, M. Rosenkranz, A. Kostanyan, T. Greber, A. U. B. Wolter, B. Büchner, A. A. Popov, *Nat. Commun.* **2017**, *8*, 16098.
[19] F. Liu, G. Velkos, D. S. Krylov, L. Spree, M. Zalibera, R. Ray, N. A. Samoylova, C. H. Chen, M. Rosenkranz, S. Schiemenz, F. Ziegs, K. Nenkov, A. Kostanyan, T. Greber, A. U. B. Wolter, M. Richter, B. Büchner, M. Stanislav S M Avdoshenko, A. A. Popov, *Nat. Commun.* **2019**, *10*, 571.
[20] B. Lefeuvre, O. Galangau, J. F. Gonzalez, V. Montigaud, V. Dorcet, L. Ouahab, B. L. Guennic, O. Cador, F. Pointillart, *Front. Chem.* **2018**, *6*, 552.
[21] Z.-X. Xiao, H. Miao, D. Shao, H.-Y. Wei, Y.-Q. Zhang, X.-Y. Wang, *Chem. Commun.* **2018**, *54*, 9726.
[22] N. Mavragani, D. Errulat, D. A. Gálico, A. A. Kitos, A. Mansikkamäki, M. Murugesu, *Angew. Chem. Int. Ed.* **2021**, *60*, 24206.
[23] E. M. Fatila, M. Rouziéres, M. C. Jennings, A. J. Lough, R. Clérac, K. E. Preuss, *J. Am. Chem. Soc.* **2013**, *135*, 9596.
[24] G. Brunet, M. Hamwi, M. A. Lemes, B. Gabidullin, M. Murugesu, *Commun. Chem.* **2018**, *88*, 1.
[25] W. R. Reed, M. A. Dunstan, R. W. Gable, W. Phonsri, K. S. Murray, R. A. Mole, C. Boskovic, *Dalton Trans.* **2019**, *48*, 15635.
[26] F. Bai, B. Yao, R. Wang, W. Wang, Q. Wang, Y. Ma, L. Li, *J. Solid State Chem.* **2021**, *298*, 122115.
[27] P. Y. Chen, M. Z. Wu, X. J. Shi, L. Tian, *RSC Adv.* **2018**, *8*, 15480.
[28] a) S. Fen, Z. Yuan, C. Jinghuo, H. Tian, C. Peng, *J. Rare Earth* **2017**, *35*, 24; b) Z.-X. Xiao, H. Miao, D. Shao, H.-Y. Wei, Y.-Q. Zhang, X.-Y. Wang, *Dalton Trans.* **2018**, *47*, 7925.
[29] L. Xi, J. Han, X. Huang, L. Li, *Magnetochemistry* **2020**, *6*, 48.
[30] S. Ma, X. Deng, M. Zhong, M. Zhu, L. Zhang, *Polyhedron* **2020**, *179*, 114370.
[31] Y. Wu, C.-C. Xia, X.-Y. Wang, *Inorg. Chim. Acta.* **2021**, *520*, 120308.
[32] J. Songa, P. Hu, L.-J. Zhang, Z.-Y. Liu, J. Yu, R.-J. Xie, L.-Z. Huang, Y.-Y. Gao, *Inorg. Chem. Commun.* **2019**, *105*, 188.
[33] a) F. Guo, R. A. Layfield, *Chem. Commun.* **2017**, *53*, 3130; b) A. Caneschi, A. Dei, D. Gatteschi, L. Sorace, K. Vostrikova, *Angew. Chem. Int. Ed.* **2000**, *39*, 246; c) C. Benelli, A. Caneschi, D. Gatteschi, L. Pardi, P. Rey, D. P. Shum, R. L. Carlin, *Inorg. Chem.* **1989**, *28*, 272.
[34] a) C. Das, A. Upadhyay, M. Shanmugam, *Inorg. Chem.* **2018**, *57*, 9002; b) J. Long, G. G. Skvortsov, A. V. Cherkasov, K. A. Lyssenko, A. I. Poddel′sky, Y. Guari, J. Larionova, A. A. Trifonov, *Dalton Trans.* **2019**, *48*, 12018.
[35] a) C. C. Lu, E. Bill, T. Weyhermüller, E. Bothe, K. Wieghardt, *J. Am. Chem. Soc.* **2008**, *130*, 3181; b) A. A. Trifonov, E. A. Fedorova, I. A. Borovkov, G. K. Fukin, V. Evguenii, E. V. Baranov, J. Larionova, N. O. Druzhkov, *Organometallics* **2007**, *26*, 2488; c) S. Zhang, W. Mo, B. Yin, G. Zhang, D. Yang, X. Lü, S. Chen, *Dalton Trans.* **2018**, *47*, 12393.
[36] a) R. Barhoumi, A. Amokrane, S. Klyatskaya, M. Boero, M. Ruben, J. .-P. Bucher, *Nanoscale* **2019**, *11*, 21167; b) E. Moreno-Pineda, E. C. Godfrin, F. Balestro, W. Wernsdorfer, M. Ruben, *Chem. Soc. Rev.* **2018**, *47*, 501; c) M. Urdampilleta, S. Klayatskaya, M. Ruben, W. Wernsdorfer, *ACS Nano* **2015**, *9*, 4458; d) S. Thiele, F. Balestro, R. Ballou, S. Klyatskaya, M. Ruben, W. Wernsdorfer, *Science* **2014**, *344*, 1135–1138; e) A. Amokrane, S. Klyatskaya, M. Boero, M. Ruben, J. .-P. Bucher, *ACS Nano* **2017**, *11*, 10750–10760; f) D. Komijani, A. Ghirri, C. Bonizzoni, S. Klyatskaya, E. Moreno-Pineda, M. Ruben, A. Soncini, M. Affronte, S. Hill, *Phys. Rev. Materials* **2018**, *2*, 024405.
[37] a) S. Alvarez, P. Alemany, D. Casanova, J. Cirera, M. Llunell, D. Avnir, *Coord. Chem. Rev.* **2005**, *249*, 1693–1708; b) P. Debye, *Ann. Phys.* **1912**, *344*, 789.
[38] a) L. F. Chibotaru, L. Ungur, *J. Chem. Phys.* **2012**, *137*, 064112; b) L. Ungur, L. F. Chibotaru, *Phys. Chem. Chem. Phys.* **2011**, *13*, 20086.
[39] a) T. Gupta, G. Rajaraman, *Eur. J. Inorg. Chem.* **2018**, *29*, 3402; b) Q.-C. Luo, Y. .-Z. Zheng, *Magnetochemistry* **2021**, *7*, 107.
[40] a) A. P. Ginsberg, *J. Am. Chem. Soc.* **1980**, *102*, 111; b) L. J. Noodleman, *Chem. Phys.* **1981**, *74*, 5737; c) L. Noodleman, E. R. Davidson, *Chem. Phys.* **1986**, *109*, 131; d) A. Bencini, D. Gatteschi, *J. Am. Chem. Soc.* **1986**, *108*, 5763; e) T. Soda, Y. Kitagawa, T. Onishi, Y. Takano, Y. Shigeta, H. Nagao, Y. Yoshioka, K. Yamaguchi, *Chem. Phys. Lett.* **2000**, *319*, 223; f) A. Bencini, F. Totti, C. A. Daul, K. Doclo, P. Fantucci, V. Barone, *Inorg. Chem.* **1997**, *36*, 5022.
[41] a) F. Aquilante, J. Autschbach, R. K. Carlson, L. F. Chibotaru, M. G. Delcey, L. De Vico, I. F. Galván, N. Ferré, L. M. Frutos, L. Gagliardi, M. Garavelli, A. Giussani, C. E. Hoyer, G. Li Manni, H. Lischka, D. Ma, P. A. Malmqvist, T. Müller, A. Nenov, M. Olivucci, T. B. Pedersen, D. Peng, F. Plasser, B. Pritchard, M. Reiher, I. Rivalta, I. Schapiro, J. Segarra-Martí, M. Stenrup, D. G. Truhlar, L. Ungur, A. Valentini, S. Vancoillie, V. Veryazov, V. P. Vysotskiy, O. Weingart, F. Zapata, R. J. Lindh, *J. Comput. Chem.* **2016**, *37*, 506; b) M. Ferbinteanu, A. Stroppa, M. Scarrozza, I. Humelnicu, D. Maftei, B. Frecus, F. Cimpoesu, *Inorg. Chem.* **2017**, *56*, 9474; c) P. -Å Malmqvist, K. Pierloot, A. R. M. Shahi, C. J. Cramer, L. J. Gagliardi, *Chem. Phys.* **2008**,

128, 204109; d) B. O. Roos, P. Taylor, P. E. M. Siegbahn, *Chem. Phys.* **1980**, *48*, 157.
[42] B. O. Roos, R. Lindh, P.-A. Malmqvist, V. Veryazov, P.-O. Widmark, A. C. Borin, *J. Phys. Chem. A* **2008**, *112*, 11431.
[43] a) B. O. Roos, P. R. Taylor, P. E. M. Siegbahn, *Chem. Phys.* **1980**, *48*, 157–173; b) P. E. M. Siegbahn, J. Almlöf, A. Heiberg, B. O. Roos, *J. Chem. Phys.* **1981**, *74*, 2384.
[44] P. A. Malmqvist, B. O. Roos, B. Schimmelpfennig, *Chem. Phys. Lett.* **2002**, *357*, 230.
[45] L. F. Chibotaru, L. Ungur, *J. Chem. Phys.* **2012**, *137*, 064112.
[46] L. F. Chibotaru *in Advances in Chemical Physics* Vol. 153, Eds.: S. A. Rice, A. R. Dinner, Wiley, 2013, pp. 397–519.
[47] L. Ungur, L. F. Chibotaru *in Lanthanides and Actinides in Molecular Magnetism*, Eds.: R. A. Layfield, M. Murugesu, Wiley-VCH, **2015**, pp. 153–184.
[48] L. Chibotaru, *Structure and Bonding* **2014**, *164*, 185.
[49] L. F. Chibotaru, L. Ungur, *The computer programs SINGLE_ANISO and POLY_ANISO*, University of Leuven, **2006**.
[50] a) L. F. Chibotaru, L. Ungur, A. Soncini, *Angew. Chem. Int. Ed.* **2008**, *47*, 4126; b) M. E. Lines, *J. Chem. Phys.* **1971**, *55*, 2977.
[51] F. Neese, Software update: The ORCA program system–Version 5.0, *WIRES-Comp Mol Sci.* **2022**, *12*, e1606.
[52] T. Gupta, T. Rajeshkumar, G. Rajaraman, *Phys. Chem. Chem. Phys.* **2014**, *16*, 14568.